

FLAME SYNTHESIS OF MgO NANOPARTICLES IN A FASP REACTOR

G. De Falco*, A. Morgan, M. Commодо***,
P. Minutolo***, A. D'Anna***

gianluigi.defalco@unina.it

* Dipartimento di Ingegneria Chimica, Università Federico II, Napoli, Italy

** Department of Chemical Engineering, Loughborough University, Loughborough, UK

*** Istituto di Ricerche sulla Combustione, C.N.R., Napoli, Italy

Abstract

The purpose of this work is the development and control of a high temperature reactor for the production of engineered nanoparticles, taking advantage from our previous studies on combustion-generated fine carbonaceous particles. The reactor consists of a laminar premixed flame, homogeneously doped with monodisperse droplets of metal precursors dissolved or dispersed in volatile solvents. The droplets are generated by a vibrating orifice aerosol generator, and injected directly into the burner. Fuel-lean and stoichiometric flames allow to produce pure metal oxide particles of nanometric sizes; by changing the flame stoichiometry to fuel-rich conditions, it is possible to obtain mixtures of metal oxide and carbonaceous nanoparticles.

Particles are collected by thermophoresis inserting a cold substrate in the flame by means of a pneumatic actuator. Morphological and dimensional analysis are performed on the collected particles by Atomic Force Microscopy (AFM) and Scanning Electron Microscopy (SEM). SEM and AFM allow inferring both qualitative and quantitative information on many physical properties including size, morphology, surface texture and roughness.

Experimental results have been obtained from a premixed stoichiometric flame of ethylene and air, doped with 75 microns droplets of magnesium nitrate hexahydrate dissolved in ethanol. Roughly monodisperse magnesium oxide particles, having a desired size ranging from 50 nm down to 4 nm, have been produced by altering the precursors concentration in the solution and the residence time of the synthesis process.

1. INTRODUCTION

Nanosized materials are playing an increasing crucial role across a wide range of applications, and new advanced techniques for the production of engineered organic and inorganic nanoparticles and their characterization are now in great demand; possible fields of use of these brand new materials range from optoelectronics to medical science. Preparation of the nanoparticles is important with respect to obtain well-defined characteristics, which in turn affects their ability to be used in different applications.

Magnesium Oxide (MgO) is one of the most useful and promising material in the field of nanosized particles; the large surface area to volume ratio and the presence of reactive sites on the surface make MgO nanoparticles suitable for uses in a number of organic heterogeneous catalyst [1]. Other possible fields of application are gas and humidity sensors and cryosurgery, due to low cost, electro-stability, nontoxic, and biodegradable properties of MgO nanoparticles.

There are many methods currently undergoing research concerning nanoparticles synthesis. Flame Assisted Spray Pyrolysis (FASP) [2] is a form of combustion aerosol synthesis based on the injection of monodisperse droplets of precursors solutions in the hot post-flame regions [3]. Compared to other techniques, which may involve costly materials or processes, FASP has the potential to be a considerably cheap, continuous production process, due to the use of inexpensive solvents (e.g. ethanol or water), and precursors such as nitrates or halides.

2. EXPERIMENTAL

2.1. FASP Reactor

The reactor, operating at atmospheric pressure, consists of a stoichiometric laminar premixed flame of C_2H_4 and air, homogeneously doped with monodisperse droplets ($75\ \mu m$) of $Mg(NO_3)_2 \cdot 6H_2O$ in ethanol solutions, at three different concentrations (4%, 6% and 8% by mass of Mg precursor). The droplets are generated by a Bergund-Liu-type Vibrating Orifice Aerosol Generator (model 345, TSI), using a $35\ \mu m$ orifice, and injected into the burner; the burner is composed by an 18 mm inside diameter (ID) stainless steel tube, with 26 mm long Mullite Zirconia Honeycomb (400 CPSI) placed on its top. The burner is heated to 410 K to ensure solvent evaporation and the feeding of the precursor metal particles directly in the high-temperature environment generated by the flame.

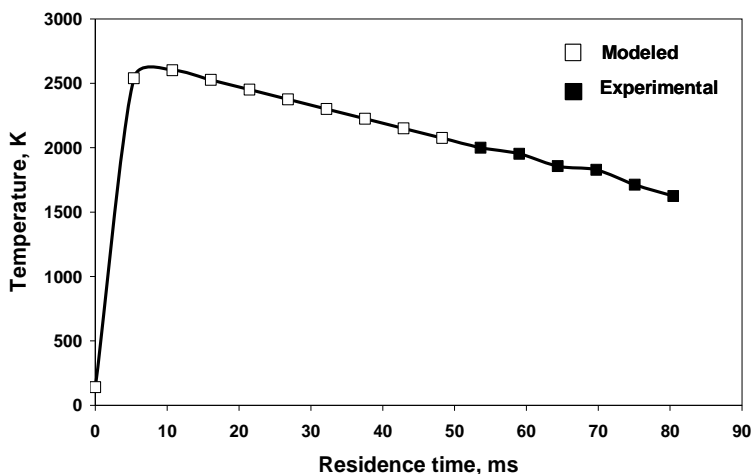


Figure 1. Flame temperature profile along the axis.

Characterization of the flame was carried out using an R-type thermocouple (Pt/13%Rh vs Pt), measuring flame temperature every centimeter above the burner down from 15 cm to 10 cm, and is reported in Fig. 1. The temperature at 10 cm reached a value (2000 K) which is above the maximum operating level of the thermocouple; therefore, temperature of the flame was modeled from 10 cm down to 1 cm using heat balances, assuming a linear decrease. Magnesium oxide particles formation in flame is attributed to the thermal decomposition mechanism of magnesium nitrate [4]; evaporation of the magnesium nitrate droplet (melting point 361.9 K; boiling point 603 K) gives free gas phase molecules of $\text{Mg}(\text{NO}_3)_2$, which then form MgO , according to the reaction: $2 \text{Mg}(\text{NO}_3)_2 \rightarrow 2 \text{MgO} + 4 \text{NO}_2 + \text{O}_2$ ($T=683 \text{ K}$).

2.2. Sampling and analysis

Nanoparticles are collected using a pneumatic actuator, able to insert different substrates in flame, assuring a constant sampling time for each insertion, ranging from 10 to 100 ms; thermophoretic forces drive particles from the hot flame toward the cold substrate, where they impact and deposit [5]. Samplings are performed at three different heights above the burner HAB (50 mm, 75 mm and 100 mm), that correspond to residence times inside the reactor of 27 ms, 40 ms and 53,5 ms.

Atomic Force Microscopy AFM (NT-MDT) analysis was performed on magnesium nanoparticles sampled on mica muscovite discs of 9 mm in diameter and 0.15 mm thick; the instrument was operated in semi-contact mode, and equipped with silicon cantilever probes (Nanosensors SSS-NCHR-20, tip diameter of 2 nm). Aluminum substrates of 9 mm in diameter were also used to collect particles for morphological analysis, by means of Scanning Electron Microscopy SEM; this technique is coupled with Energy-Dispersive X-Ray Spectrometry, in order to obtain the chemical composition of the samples.

3. RESULTS AND DISCUSSION

Samples for SEM analysis were obtained by thermophoretic collection performed with high insertion times, greater than 50 ms, due to the low magnification of the instrument in the nanoscale and the need for large particles for elemental composition analysis. This has led to high residence time of the substrate in the flame, and so particles growth occurred on the substrate, producing SEM images of large particle agglomerates, surrounded by a layer of particles of sizes below that of the instrumental resolution. Occasionally single micron spherical particles. As shown in Fig. 2, are found on the samples with shorter insertion times of 50 ms and a single insertion. Magnesium (Mg), Oxygen (O) and Nitrogen (N) are found to be present in the EDXS analysis of these particles.

The AFM results produced 2D and 3D topological maps, with a resolution down to 1 nm^3 . The optimal insertion time to collect by thermophoresis an appropriate number of isolated particles was found to be equal to 30 ms; longer insertion times could induce coalescence phenomena on the substrate, while shorter insertion times

don't allow to collect enough particles for microscopy analysis. AFM images were then analyzed to obtain volume, base area and maximum height above the mica of the particles.

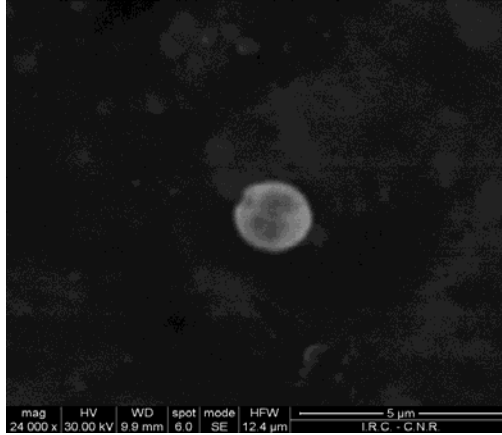


Figure 2. SEM image of a MgO spherical particle after a single insertion at 50 ms, HAB=100 mm, Mg Nitrate concentration=6%.

The equivalent diameters ED, defined as the diameter of a sphere of equivalent volume, were calculated, and the AFM data were converted to ED normalized frequency distributions; the latter was then fitted by two lognormal distribution functions [6], shown in Equation 1, where ED is the particle diameter, D_p is the particle median diameter, N is the number density of the particles, σ is the geometric standard deviation, and w is particle number fraction.

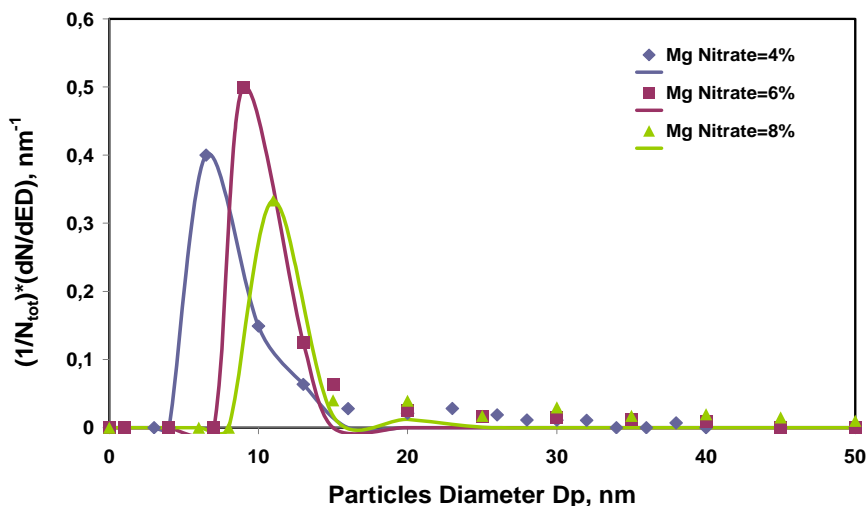
$$\begin{aligned} \frac{1}{N} \frac{dN}{ED} = & \frac{w}{ED \sqrt{2\pi} \ln(\sigma_1)} \exp \left(- \frac{(\ln(ED) - \ln(D_{p1}))^2}{2 \ln(\sigma_1)^2} \right) + \\ & + \frac{1-w}{ED \sqrt{2\pi} \ln(\sigma_2)} \exp \left(- \frac{(\ln(ED) - \ln(D_{p2}))^2}{2 \ln(\sigma_2)^2} \right) \end{aligned} \quad (1)$$

The parameters used to fit the size distributions function, obtained at three different HAB (50 mm, 75 mm, 125 mm) for all the three concentrations (4%, 6%, 8% of Mg precursors), are reported in Table 1. The geometric standard deviation ranged from a minimum of 1,01 to a maximum of 2,12; for increasing HAB and thus residence times, there was a noticeable increase of particle sizes. All three concentrations exhibit some bimodal size distributions with in increasing HAB; for higher concentrations, the bimodal nature of the size distributions is more pronounced

Table 1. Parameters used to fit the AFM log normal size distribution functions.

Mg%	HAB (mm)	Mean Diameter (nm)		Standard Deviation		First mode weight
		$\langle D_{p1} \rangle$	$\langle D_{p2} \rangle$	σ_1	σ_2	w
4%	50	6.98	10.6	1.05	1.11	0.85
	75	9.1	29.6	2.12	1.2	0.75
	100	14.13	40	1.29	1.23	0.622
6%	50	9.41	12.8	1.01	1.19	0.8
	75	12.12	31.72	1.37	1.38	0.55
	100	16.49	42.33	1.54	1.3	0.72
8%	50	10.3	18.53	1.04	1.16	0.8
	75	13.54	33.85	1.06	1.5	0.62
	100	17.3	45	1.22	1.77	0.59

Fig. 3 shows particles size distributions obtained at HAB=50 mm, corresponding to a residence time inside the reactor of 27 ms, for the three concentrations; points represent the AFM experimental data, while lines are their best fitting. As can be seen, mostly monodisperse particles with mean sizes of 7 nm, 9,5 nm and 11 nm can be obtained.


Figure 3. Particles size distributions at HAB=50 mm.

Particles aspect ratio AR was measured as a function of the particles equivalent spherical diameter; AR was calculated as the maximum height of the isolated particle divided by its base diameter. The results are shown in Fig. 4 for 8% concentration of Mg precursors; a similar trend of results was found for each concentration and residence time.

The low calculated aspect ratio, between 0.1 and 0.8, can be attributed to a plastic behavior of the nanoparticles inside the flame, which are subjected to a deformation when colliding on the substrate [7]. Greatest particles exhibit the highest values of aspect ratio, probably due to a less plastic nature with respect to smaller particles.

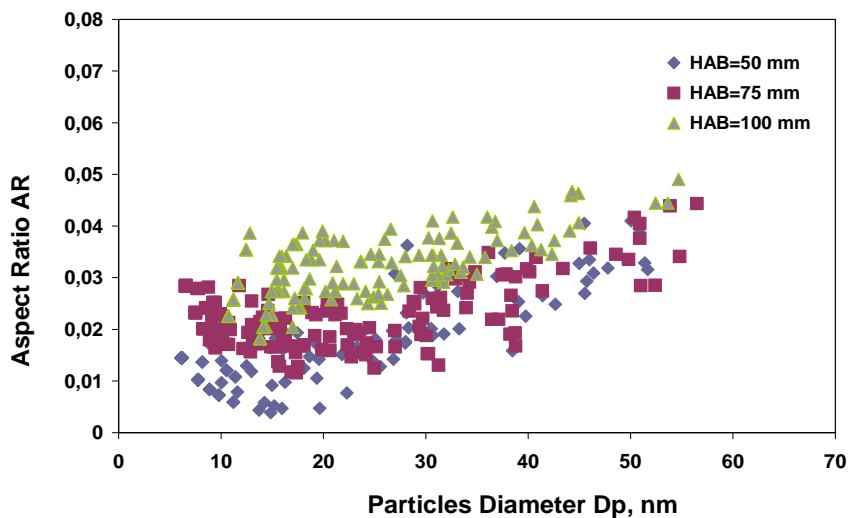


Figure 4. Particles aspect ratio, Mg Nitrate concentration=8%.

4. CONCLUSIONS

Magnesium oxide nanoparticles were successfully produced using Flame Assisted Spray Pyrolysis in a high temperature reactor; it has been found that residence time and precursor concentration influences the sizes of the formed nanoparticles. At a residence time of 23 ms, almost monodisperse particles with mean sizes between 7 and 11 nm can be obtained, by varying the precursor concentration in the solution droplets. Engineered nanoparticles of pure metals and metal oxides, or mixtures of metals and carbonaceous compounds can be obtained easily with this apparatus by changing the flame stoichiometry and the fuel characteristics.

Acknowledgements

The authors wish to thank Dr. Luciano Cortese of Istituto di Ricerche sulla Combustione in Naples for the help in performing and understanding SEM measurements.

References

- [1] Ganguly, A., Trinh, P., Ramanujachary, K.V., Ahmad, T. and Mugweru, A., "Reverse micellar based synthesis of ultrafine MgO nanoparticles (8–10 nm): Characterization and catalytic properties", *Journal of colloid and*

- interface science*. 353: 137-142 (2011).
- [2] Strobel, R., Baiker, A. and Pratsinis, S.E., "Aerosol flame synthesis of catalysts", *Adv. Powder Technol.* 17(5): 457-480 (2006).
 - [3] D'Anna, A., Kurz, M. and Merola, S.S., "Particle Formation from Single Droplets of Aqueous Solutions of Lead Nitrate", *Part. Part. Syst. Charact.* 15(5): 237-242 (1998).
 - [4] Mu, J. and Perlmutter, D.D., "Thermal decomposition of metal nitrates and their hydrates", *Thermochimica Acta* 56: 253-260 (1982).
 - [5] Sgro, L.A., Barone, A.C., Commoco, M., D'Alessio, A., De Filippo, A., Lanzuolo, G. and Minutolo, P., "Measurement of nanoparticles of organic carbon in non-sooting flame conditions", *Proc. Comb. Inst.* 32: 689-696 (2009).
 - [6] Hinds, W. C., *Aerosol technology: properties, behavior and measurements of airborne particles*, Wiley-Interscience, New York, 1999.
 - [7] Barone, A.C., D'Alessio, A. and D'Anna, A., "Morphological characterization of the early process of soot formation by atomic force microscopy", *Combust. Flame* 132: 181-187 (2003).